

# Experimental study on the mechanical behavior of polypropylene fibre reinforced concrete subjected to monotonic loads

Eduardo Nuñez-Castellanos<sup>a\*</sup> , Ronald Torres-Moreno<sup>b</sup>, Salvador Ligas-Fonseca<sup>b</sup>,  
Guillermo Bustamante-Laissle<sup>a</sup>, Nelson Maureira-Carsalade<sup>a</sup> , Angel Roco-Videla<sup>c,d</sup> 

<sup>a</sup> Departamento de Ingeniería Civil, Universidad Católica de la Santísima Concepción, Alonso de Ribera 2850, Concepción-Chile. Email: enunez@ucsc.cl, gbustamante@ucsc.cl, nmaureira@ucsc.cl

<sup>b</sup> Instituto de Materiales y Modelos Estructurales, Facultad de Ingeniería, Universidad Central de Venezuela, Caracas 1051, Venezuela. Email: ronald.torres@ucv.ve, salvador.ligas@ucv.ve

<sup>c</sup> Facultad de Salud, programa de Magíster en Ciencias Químico-Biológicas, Universidad Bernardo O'Higgins, General Gana 1702, Santiago-Chile. Email: angelroco@postgrado.ubo.cl

<sup>d</sup> CAMIPER, Escuela de altos estudios, Camara Minera del Perú, Los Canarios 105, Lima-Perú. Email: aroco@grupocamiper.org

\* Corresponding author

<https://doi.org/10.1590/1679-78256638>

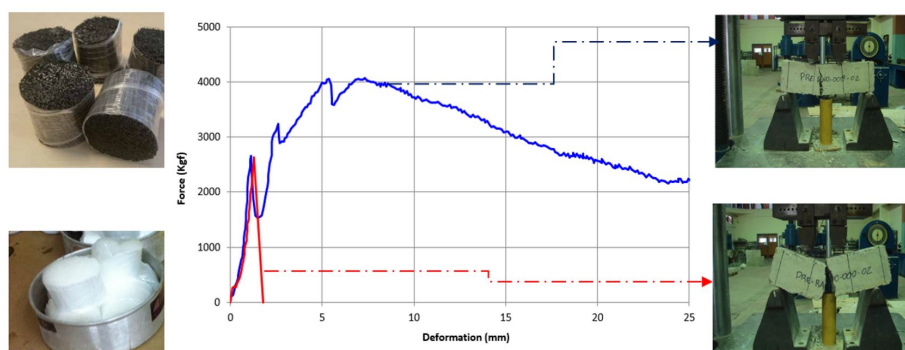
## Abstract

The properties of fibre reinforced concrete were studied under monotonic loads according to Japanese, North American and European codes. Two different types of SIKA polypropylene fibre were with different dosages. One hundred and eighty tests were performed, obtaining resistance to compression, tension, bending, toughness, and energy absorption in the hardened state. The results show that the addition of fibres affects the workability of the concrete mix. The increase in fibre dosage does not affect compressive, tensile, or flexural strength. However, the failure changes from brittle to more ductile, allowing it to reach residual strengths of 50% of the maximum reached and 200% deformation. The dissipated energy increased with increasing fibre dosage. The performance achieved by both fibres was similar, although the optimal dosage was 6 kg/m<sup>3</sup> for type A fibres and 8 kg/m<sup>3</sup> for type B. Therefore, the replacement of flexural reinforcing steel in the foundation slabs of one-story buildings can be performed if adequate dosages are used in compliance with established analytical procedures for industrial floor design.

## Keywords

Fibre reinforced concrete, polypropylene fibres, compressive strength, toughness, dissipated energy.

## Graphical abstract



Received July 02, 2021. In revised form October 01, 2021. Accepted October 04, 2021. Available online October 06, 2021.

<https://doi.org/10.1590/1679-78256638>



Latin American Journal of Solids and Structures. ISSN 1679-7825. Copyright © 2021. This is an Open Access article distributed under the terms of the Creative Commons Attribution License, which permits unrestricted use, distribution, and reproduction in any medium, provided the original work is properly cited.

## 1 INTRODUCTION

The use of fibre in construction materials dates back to the Neolithic age, where, together with the cob, adobe and straw were used to increase the tensile strength of elements. Currently, there are steel, glass, synthetic, carbon, and natural fibres in the construction industry that are used with the same principle. Additionally, its structural performance depends mainly on the tensile strength and the dosage of the fibre, being important to characterize the mechanical behavior for each type of fibre to be used. The fibres provide bridging and confinement of the cracks in the failure plane to considerably improve energy absorption capacity. However, a higher dosage of fibres reduces workability and compressive strength. Studies show that steel fibres provide superior performance to a similar dose of other fibres. However, corrosion can condition the durability of elements reinforced with steel fibres, which is why the use of other types of fibres such as synthetic is recommended when this is a problem (Costa et al., 2018).

Fibre concrete has been used in various applications, the most frequent being constructing high-performance industrial floors, pavements, bridge decks, shotcrete for slope stabilization, tunnel lining, precast structural elements, and vaults, among others. Mendoza et al. (2011) studied the influence of a type of polypropylene fibre on the properties of concrete in plastic and hardened states, determining the effect that the incorporation of short polypropylene fibres has on its properties. Eight mixtures were manufactured, which were tested in the fresh state and at the ages of 7 and 28 days, with fibre dosages of 1, 3 and 5 kg/m<sup>3</sup>. Air content and cracking due to plastic shrinkage were determined to the concrete in the fresh state, while in the hardened state, toughness and resistance to compression, tension and impact were obtained. The results showed that the fibres in fresh concrete reduce plastic shrinkage cracking, while in the hardened state, it increases toughness and impact resistance. In addition to reducing drying shrinkage and cracking, the rest of the variables studied did not show significant changes.

Zheng et al. (2020) conducted laboratory tests to explore the effects of fibre dosage on the mechanical properties and failure modes of reinforced concrete. Samples with different dosages (0 wt%, 0.4 wt%, 0.8 wt%, or 1.2 wt%; wt=weight fraction) and fibre types (polypropylene, glass and polyacrylonitrile) were prepared and subjected to uniaxial compression tests. Before and after each test, a computerized industrial scan (CT) was carried out on each sample in order to analyze the evolution in time and space (deformation in time) of the internal microcracks. The experimental results showed that the uniaxial compressive strength in fibre reinforced concrete initially increases and decreases as the fibre dosage is increased. The maximum tensile strength of the glass fibre reinforced concrete was greater than that of the polypropylene and polyacrylonitrile fibre reinforced samples. The maximum stress in concrete with 0.8 wt% fibreglass exceeded the maximum stress of ordinary concrete by 39%. The deformation of fibre reinforced concrete increased linearly with increasing fibre dosage. The extent of the bridging effects (adhesion, bonding) of the three types of fibre in concrete cracks can be classified in decreasing order as fibreglass > polypropylene fibre > polyacrylonitrile fibre, according to the results of computerized industrial scanning.

Abdelmajeed, W. (2020) studied the influence of hybrid steel-polypropylene fibres in improving the punching capacity in the slab-column connection. An experimental program was adopted to evaluate the influence of hybrid fibre on punch cutting as a key property in a concrete member. The results showed a significant improvement in the punching ability of the concrete samples with hybrid fibres compared to the single fibre concrete mixes. The improvement was observed even in other concrete properties such as compressive and flexural strength, crack behavior, ductility and toughness.

Xu et al. (2020) addressed a study of the mechanical properties of concrete reinforced with cellulose fibre (CTF), polyvinyl alcohol fibre (PF) and polyolefin fibre suitable for various sprinklers (VS). The individual impact of a single fibre was investigated, as well as the synergistic effect of hybrid fibre on axial compressive strength, tensile strength at break, and shear strength. The results showed that the CTF individually improves the strength of concrete to axial compression, but weakens the tensile strength at break. The VS fibre weakens the tensile strength by breaking, having a small impact on the other two strengths. PF has a negative effect on all three resistance mechanisms.

Usman (2020) evaluated the effect of the natural action of weathering in prestressed concrete beams. These consist of a control or reference mix, two steel fibre reinforced concrete (SFRC) beams, two with polypropylene fibre reinforced concrete (PPFRC) and one with both fibres. The samples were subjected to natural exposure to the open atmosphere for 36 months. The durability properties studied include unit weight, compressive strength, water absorption, porosity, chloride penetration test, scanning electron microscope analysis, and energy scattering X-ray analysis. It was concluded that, by exposure to natural weather, polypropylene fibres improve durability and cancel out the effect of steel fibres in hybrid fibre reinforced concrete. The behavior and response of concrete reinforced with polypropylene macrofibre after cracking has been investigated by Amin et al., (2017) by conducting direct and indirect tensile tests. The results showed an increase in cracking recorded for the fibre specimens, the round panel test being the one that showed the least variability. Finally, an empirical formula is proposed to obtain the Strength of concrete reinforced with fibres.

A numerical and experimental study on behaviour of macro-synthetic fibres reinforced concrete was performed by Nana et al. (2021). The influence of the fibre dosage was evaluated with dosages of 3.0, 4.5, 6.0, 7.5, 9.0 and 11.5 kg/m<sup>3</sup>. The results obtained showed an increase in the residual tensile flexural stresses. A numerical model using the inverse method was also used to reproduce the stress/crack opening behaviour of FRC obtained in the experimental tests. In Hao & Hao (2013), the dynamic compressive properties of spiral fibre reinforced concrete were conducted. Specimens with different volume fractions of spiral fibres ranging from zero to 1.5% were tested. The results obtained showed that the compressive and tensile strengths, material ductility, and energy absorption capability of steel fibre reinforced concrete increase with the volume fraction of spiral fibres. The experimental study on the effect of high strain rate on compressive behavior of plain and fibre-reinforced high-strength concrete with strength between 80-90 MPa was conducted by Wang et al. (2012). The compressive strength, elastic modulus, critical strain, and toughness of the concrete were increased with strain rate. The deflection of reinforced concrete beams with recycled steel fibres was studied by Fantilli et al. (2021). In specimens with a low dosage of fibres, there is a reduction in deflections and the load at yielding of steel increases with the content of fibres. On the contrary, the mechanical behavior of R/FRC and RC beams does not substantially differ in the presence of a highly effective reinforcement ratio.

In the study conducted by Fan et al. (2020), the shrinkage and fracture properties of superabsorbent polymers (SAP) modified concrete with and without hybrid fibres were investigated. The results showed that compared with that of SAP modified concrete, the fracture energy was increased, and the total cracking per unit of area was reduced. The addition of both the hybrid fibre and SAP significantly reduced the shrinkage of the concrete, mainly by decreasing the shrinkage rate of the concrete and accelerating the time required for the concrete shrinkage to stabilize. According to research performed by Nogales and de la Fuente (2021), a numerical study based on the finite element method was implemented and validated by means of results from existing full-scale tests. The structural efficiency of the fibre reinforced concrete elements is more noticeable when low residual strength classes are considered. On the other hand, the structural response of a fibre reinforced concrete pile-supported flat slab was conducted by means of full-scale tests (Aidarov et al., 2021). The results obtained in this experimental program represent new evidence of the structural suitability of the SFRC in a pile-supported flat slab, even with total substitution of the longitudinal steel bars. In Wang et al. (2021), the static and flexural fatigue performance of ultra-high performance fibre reinforced concrete (UHPRC) slabs were studied. In contrast to straight steel fibers, the results showed that the use of hooked-end steel fibres could have a better advantage to increase the crack resistance and post-cracking stiffness of the deck specimens. Due to the use of steel fibres and steel bars, cracks in the UHPRC deck specimens propagated rather slowly under both static and fatigue loads.

In the research performed by Junaid et al. (2021), the addition of macro-polypropylene fibres improves the stress-strain performance of natural aggregate concrete (NAC). However, limited studies focus on the stress-strain performance of macro-polypropylene fibre-reinforced recycled aggregate concrete (RAC). Considering the variability of coarse recycled aggregates (CRA), more studies are needed to investigate the stress-strain performance of macro-polypropylene fibre-reinforced RAC. The negative effect of CRA on the properties of concrete samples can be minimized by adding BarChip macro-polypropylene fibres. The applicability of the stress-strain model previously developed for macro-synthetic and steel fibre-reinforced NAC and RAC to BFAC and BFRAC is also examined. In the investigation performed by Camille et al. (2020), the evaluation of macro-synthetic fibre reinforced concrete (MSFRC) structural performances under both static and dynamic loadings was studied. The results showed that the macro-synthetic fibre reinforcement can improve the durability of concrete and reduce the damage caused through thermal cycles. In the tests performed, the fibre reinforced concrete has been proposed to minimize the static and dynamic failure modes while as anticipated, improve the post-cracking behaviour. It is a common perception that fibre reinforced concretes (FRC) are prone to internal and external deterioration due to the presence of these. This fact is the reason why the construction industry is reluctant to use FRC (except for steel bar reinforcement) despite having a host of advantages.

The experimental study carried out by Baarimah and Moshin (2017) shows the behavior of concrete slabs with steel fibres for different dosages by testing six reinforced concrete slabs. The results obtained show a change in the failure mode from brittle to ductile and allows a reduction in the thickness of the slabs. On the other hand, a numerical and experimental investigation carried out by (Cajka et al., 2020a) studied the behavior of four concrete slabs reinforced with steel fibre. Different types of tests can be performed to evaluate the behavior of fibre-reinforced concrete elements (Cajka et al., 2020b). Basic tests such as compression and traction make it possible to obtain basic properties such as modulus of elasticity and resistance according to the type of applied stress. The bending tests in beams or slabs allow to obtain the flexural strength, toughness and absorbed energy, these tests being the most significant because they show the contribution of resistance of the fibre in the structural element, completely modifying its behavior. Finally, there are the real-scale tests of elements such as slabs that allow evaluating additional aspects such as the soil-structure interaction and its incidence with the characteristics of the element. However, these latter trials are expensive and require the use

of more complex equipment (Cajka et al., 2020a). For this reason, in this research, a numerical modeling was carried out incorporating the constitutive law of fibre-reinforced concrete, previously obtained from the tests carried out, to evaluate the performance of the foundation slab numerically. The results show that slabs with higher dosages achieve higher deformations and are capable of supporting higher loads.

Numerical models using FE, especially incorporating nonlinear analysis, are currently an effective tool for optimization in structural design (Cajka et al., 2020 b). However, the designs are often limited by insufficient information on the materials used, which is essential to establish constitutive laws from tests when a fibre-reinforced concrete is used. The fibres currently used in the market show the results of tests carried out in the laboratory under controlled conditions. However, field conditions introduce uncertainties that modify actual performance. For this reason, in this research, a concrete from a ready-mix concrete company is used, adding the fibre once the concrete arrives at the work, trying to simulate the conditions to which the concreting of the foundation slabs is subjected.

The effect of the variety of fibre types available on the design parameters needs to be evaluated, and its standardization is one of the most difficult aspects in the design process (Zollo, 1997). In addition, the fibres provide adhesion bridges that allow the distribution of internal forces and considerably improve the toughness and energy absorption capacity, allowing control of the fracture (Zollo, 1997).

Specifically, this research proposes to characterize the behavior of reinforced concrete with polypropylene macro-fibres from the obtaining of mechanical properties. Additionally, the implementation of the results obtained in the flexural design of foundation slabs in low-cost homes will be evaluated using reinforced concrete with two types of fibre (Fibre type A and fibre type B, both commercialized by SIKA) as an alternative to the use of reinforcing steel using analytical methods and its comparison with a numerical simulation in finite elements.

## 2 EXPERIMENTAL PROGRAM

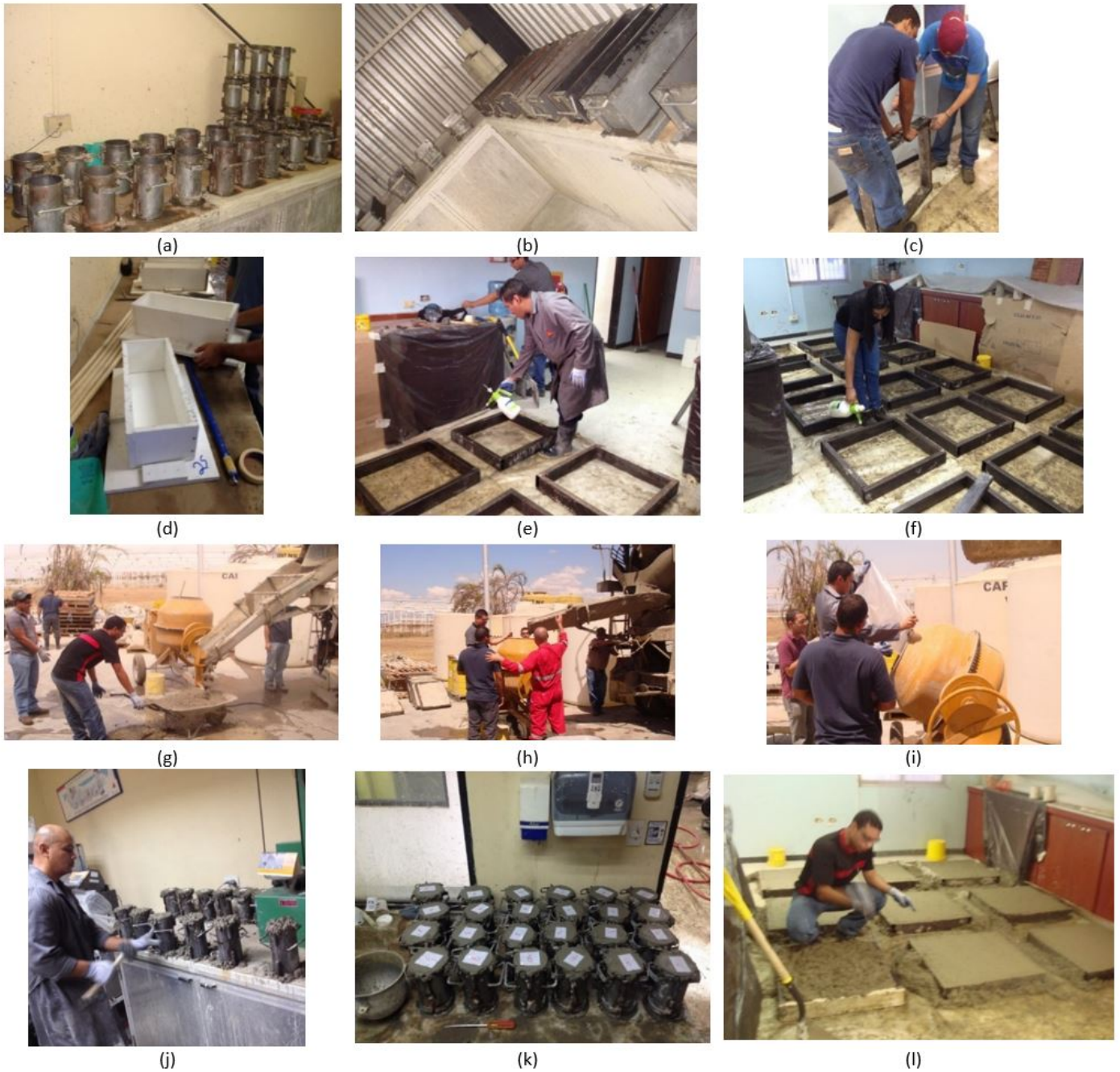
The experimental study was carried out on concrete samples with two types of non-fibrillated monofilament polypropylene fibre belonging to the company SIKA (for commercial reasons, the names of each fibre will not be specified). Type A fibre has a length  $L=55\text{mm}$ , diameter  $\phi=0.65\text{mm}$  (circular cross section) and tensile strength  $\sigma=360\text{MPa}$ . Type B fibre has a length  $L=55\text{mm}$ , an average width of  $1.2855$  with an average thickness of  $0.3325\text{mm}$  (rectangular cross section) and tensile strength  $\sigma=550\text{MPa}$ . The tests to be carried out for the validation of the following research are grouped into two stages: i) for concrete in a fresh state, Settlement test according to ASTM C143 / C143M (2020), temperature test according to C1064 / C1064M (2017), air content according to ASTM C231 / C231M (2017) and density test according to ASTM C138 / C138M (2019); ii) for concrete in hardened state, compression test of cylinders according to ASTM C39 / C39M (2020), indirect tensile test of cylinders according to ASTM C496 / C496M (2017), flexural strength and flexural toughness according to JSCE-SF4 (1984), flexural strength according to ASTM C1609 / C1609M (2019) and energy absorption test according to EFNARC (1996).

For each type of test, three measurements were made on three different specimens made in the SIKA-Venezuela laboratories. The fibres used will be called TYPE A and TYPE B, and the concrete was specified for a compressive strength of  $28\text{MPa}$ , whose coarse aggregate will not exceed a nominal size of  $25\text{mm}$ . The fibre dosages to be used will be:  $0, 4, 5, 6, 7$  and  $8\text{ kg/m}^3$  of concrete. The behavior between the standard sample ( $0\text{ kg/m}^3$  of fibre) and the samples with different fibre dosages will be compared. According to the before mentioned tests, a total of 180 specimens were made and distributed, as shown in Table 1 by type of fibre.

**Table 1** Specimens tested for Fibre type A and Fibre Type B

Experimental test	Specimen dimension	Dosage by Fibre type					
		0 kg/m <sup>3</sup>	4 kg/m <sup>3</sup>	5 kg/m <sup>3</sup>	6 kg/m <sup>3</sup>	7 kg/m <sup>3</sup>	8 kg/m <sup>3</sup>
Compression according to ASTM C39	Cylinder ( $\phi 100 \times 200\text{ mm}$ )	3	3	3	3	3	3
Indirect Tension according to ASTM C496	Cylinder ( $\phi 100 \times 200\text{ mm}$ )	3	3	3	3	3	3
Flexural according to ASTM 1609	Beam ( $150 \times 150 \times 500\text{ mm}$ )	3	3	3	3	3	3
Flexural according to JSCE SF4	Beam ( $100 \times 100 \times 350\text{ mm}$ )	3	3	3	3	3	3
Energy absorption according to EFNARC	Slab ( $600 \times 600 \times 10\text{ mm}$ )	3	3	3	3	3	3
	Sub-total	15	15	15	15	15	15
	Total	90					

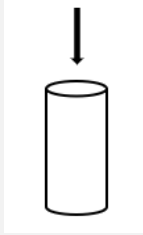

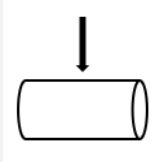

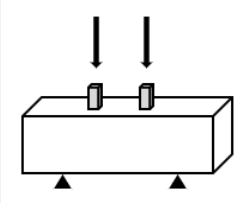

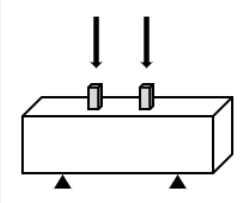

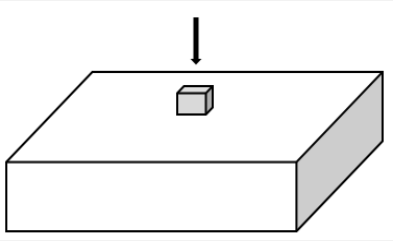

In Figure 1, the stages of the manufacture of specimens and concreting of the specimens to be tested are shown. The cylinders, boxes and steel frames used as molds were duly prepared according to what is established in the different standards used, as shown in Figure 1a-1b-1c-1d-1e-1f. Figures 1g-1h-1i show stages during the reception of ready-mixed concrete, and Figures 1j-1k-1l show the stage of making the specimens.



**Figure 1:** Preparation and making of cylindrical, rectangular and flat specimens for testing

The Table 2 shows a diagram of each test carried out in the hardened concrete phase and the instrumentation used.

**Table 2** Scheme and parameters in tests

View of scheme	View of test	Parameters
		<p>Test: ASTM C39                      Dimensiones: diameter = 100mm and height = 200mm                      Parameter: compressive strength                      Instrumentation: celd load and LVDT, incorporated in test machine.</p>
		<p>Test: ASTM C496                      Dimensiones: diameter = 100mm and height = 200mm                      Parameter: tensile strength                      Instrumentation: celd load and LVDT, incorporated in test machine.</p>
		<p>Test: ASTM C1609                      Dimensiones: width = 150mm, height = 150mm and length =500mm                      Parameter: flexural strength                      Instrumentation: celd load and LVDT, incorporated in test machine.</p>
		<p>Test: JSCE-SF4                      Dimensiones: width = 100mm, height = 100mm and length =350mm                      Parameter: flexural strength                      Instrumentation: celd load and LVDT, incorporated in test machine.</p>
		<p>Test: EFNARC                      Dimensiones: width = 600mm, thickness = 100mm and length =600mm                      Parameter: Dissipated energy                      Instrumentation: celd load and LVDT, incorporated in test machine.</p>

**3 RESULTS OF EXPERIMENTAL PROGRAM**

**3.1 Settlement according to ASTM C143**

The settlement is an important parameter during the construction of a work. Low settlements make it difficult to distribute the concrete in the structural elements, favoring the voids. Fibre-reinforced concretes can be affected when

the dosage increases. The Figure 2 shows the settlements obtained according to ASTM C143 / C143M (2020), in relation to the settlement of the mixture without fibre, according to the different dosages in the fresh state. The results show that the higher the dosage of fibre in the concrete, the lower the measured slump, reaching up to 34% reduction for TYPE A fibre and up to 47% for TYPE B fibre. The initial slump for the mix with TYPE fibre A reached 9.5 inches, and for the TYPE B fibre mix, it reached 6.5 inches. The concrete's workability loss is due to the increase of the internal cohesion of the components of the mixture, being an important parameter to consider when concrete with fibre is specified in civil works.

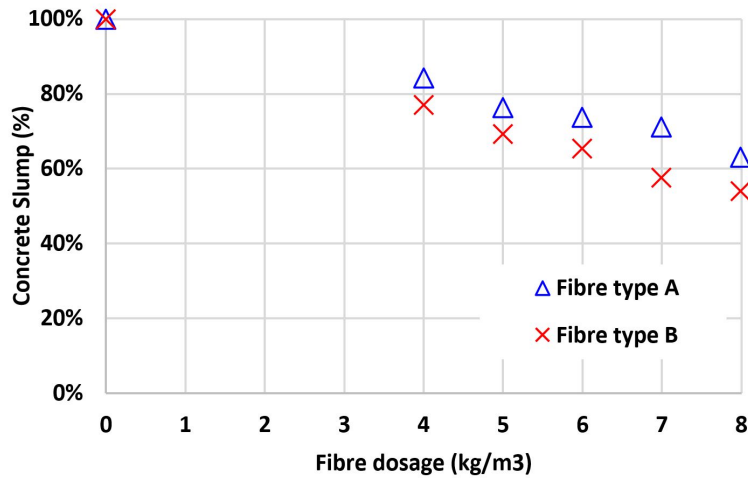


Figure 2: Slump variation in tested samples

### 3.2 Temperature according to ASTM C1064

Figure 3 shows the variation of the temperature of the concrete in the fresh state according to ASTM C1064 / C1064M (2017) when fibres are added. The results show a slight rise in temperature. However, this elevation is due to the exothermic chemical reaction process of the concrete. This behavior was obtained for the two types of fibres studied. The preparation of the test tubes was carried out in a time interval of one hour and a half, taking approximately 10 minutes for the preparation of all the samples corresponding to a dosage.

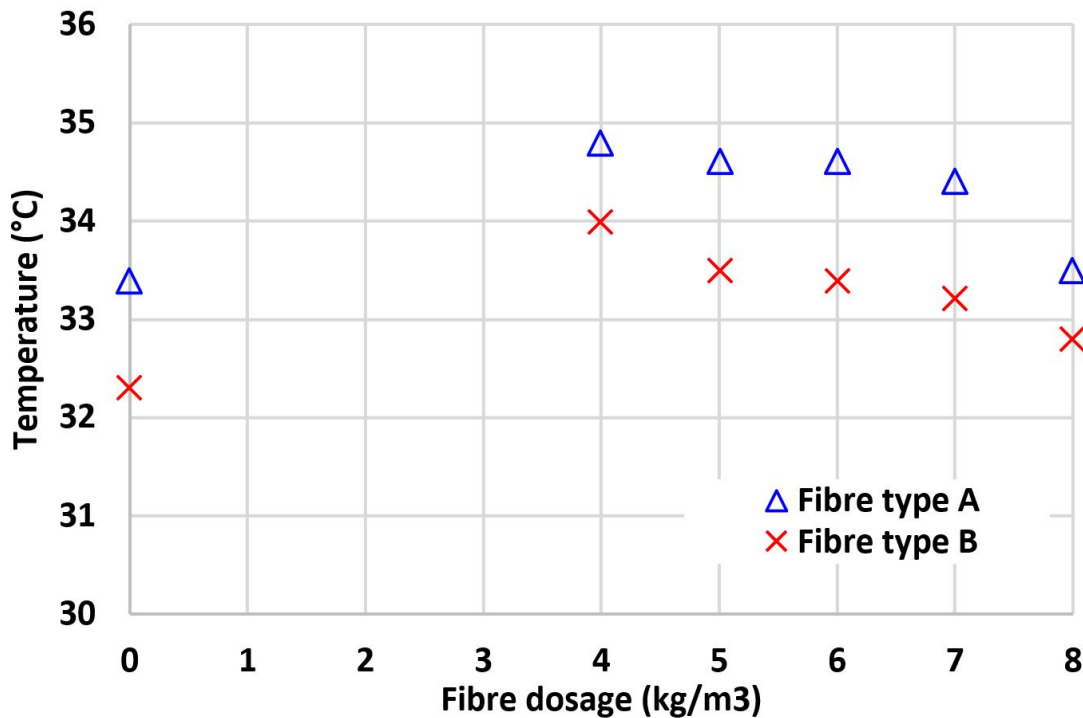


Figure 3: Temperature variation in tested samples

### 3.3 Air contained according to ASTM C231

The fibres during their incorporation into the concrete mix can increase the amount of air, especially at the microstructure level, affecting the porosity and durability of the element (Zollo, 1997). The Figure 4 shows the percentages of air contained in the concrete in a fresh state according to ASTM C231 / C231M (2017) and ASTM C138 / C138M (2019). The results show no variation as the dosage of fibre in the concrete increases. This behavior was similar for the two types of fibres used. The air content observed in both mixtures is within the limit recommended by the ACI 318-14 (2014) standard of 4% to guarantee a concrete without entrapped air.

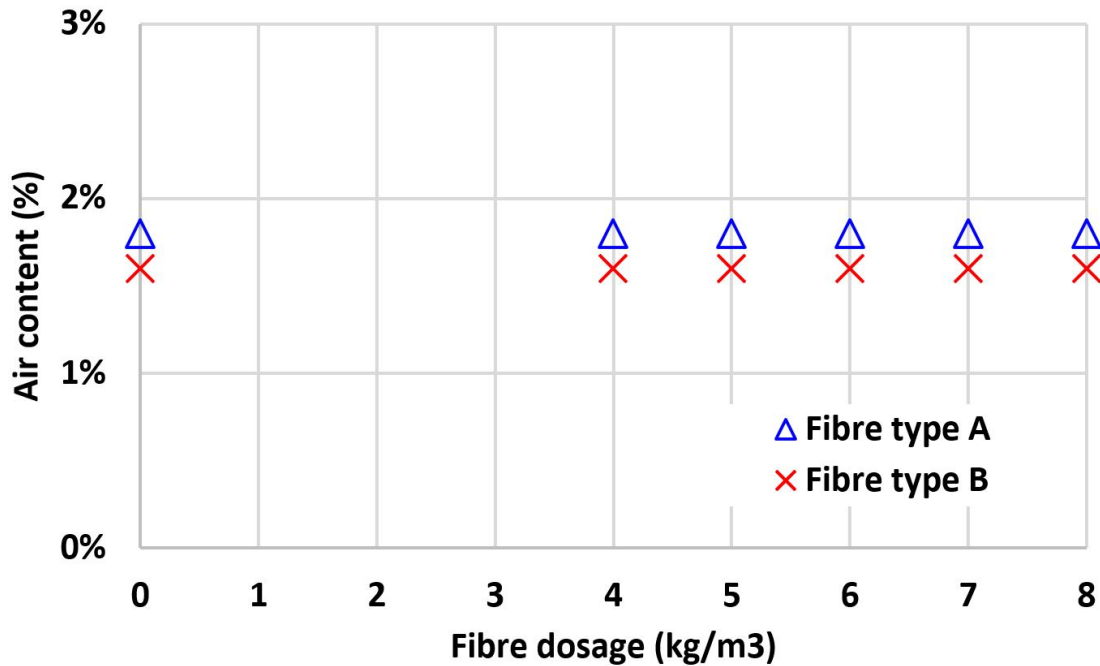
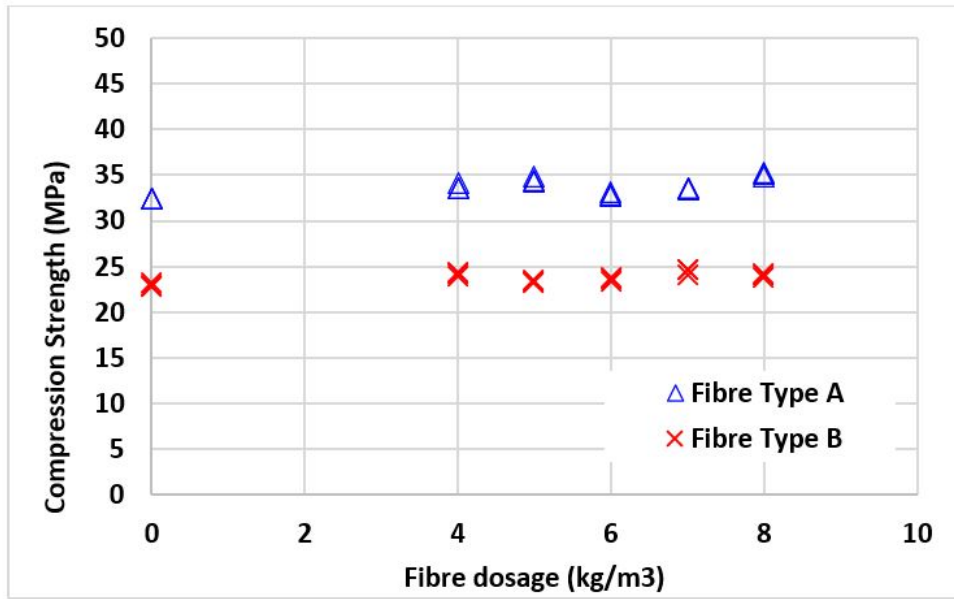


Figure 4: Variation of the air contained in tested samples

### 3.4 Compressive Strength according to ASTM C39

The Compressive Strength  $f_c = P_{max}/A_c$  is obtained by dividing the maximum compression load by the cross-sectional area of the tested cylinder. The Figure 5a shows the compressive strength of concrete according to ASTM C39 / C39M (2020) obtained for the different specimens in all their dosages with fibre A and B. The results obtained are different between the different specimens; therefore, there is no trend or repeatability. Thus, there is no relationship between the loss of compressive strength and the amount of fibre added, at least in the dosages tested. The standard deviation obtained was 0.94 MPa for the mixture with type A fibre and 0.52 MPa for the mixture with type B fibre. This was a low dispersion in the results obtained, with coefficients of variation of 2.80% and 2.21%, respectively. An increase in compressive strength is observed; however, this increase is not related to the dosage of fibre added to the mixture since there are cases in which the resistance obtained is lower with higher dosages. For example, for type A fibre, the resistance of cylinders with a dosage of 7 kg/m³ is lower than the resistance of the cylinders with a dosage of 5 kg/m³. In figures 5b and 5c, the forms of failure in the cylinder with fibre and without added fibre are observed, respectively. The presence of fibre prevented disintegration of the tested sample, improving the form of failure. This fact is due to the bridges generated by the added fibre.





(a)



(b)

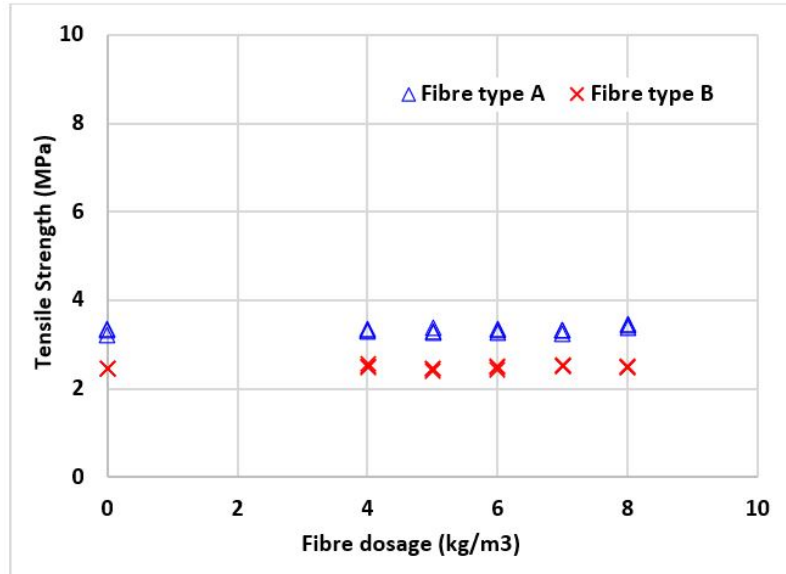


(c)

**Figure 5:** (a) Variation of compressive strength in specimens with TYPE A fibre and TYPE B fibre, (b), (b) compression failure in specimens with fibre, (c) compression failure in specimens without fibre.

### 3.5 Tensile strength according to ASTM C496

The Tensile Strength  $T = 2P_{max}/\pi ld$  is obtained by dividing the maximum compression load by the cross-sectional area of the tested cylinder. In Figure 6a the tensile strength is shown according to ASTM C496 / C496M (2017) obtained for the different specimens in all their dosages for fibre types A and B. The results obtained show a variation between the different specimens. However, there is no trend or repeatability. Therefore, there is no relationship between the loss of tensile strength and the amount of fibre added, at least in the dosages tested. The standard deviation obtained was 0.063 MPa for the mixture with type A fibre and a standard deviation of 0.032 MPa for the mixture with type B fibre, being a low dispersion in the results obtained, with some coefficients variation of 1.92% and 1.33% respectively. In Figures 6c and 6d, the forms of failure in the cylinder with fibre and without added fibre are observed, respectively. The presence of fibre prevented, like the compression test, a disintegration of the tested sample. This outcome again shows the bridges generated by the added fibre in the tested mixtures.



(a)



(b)

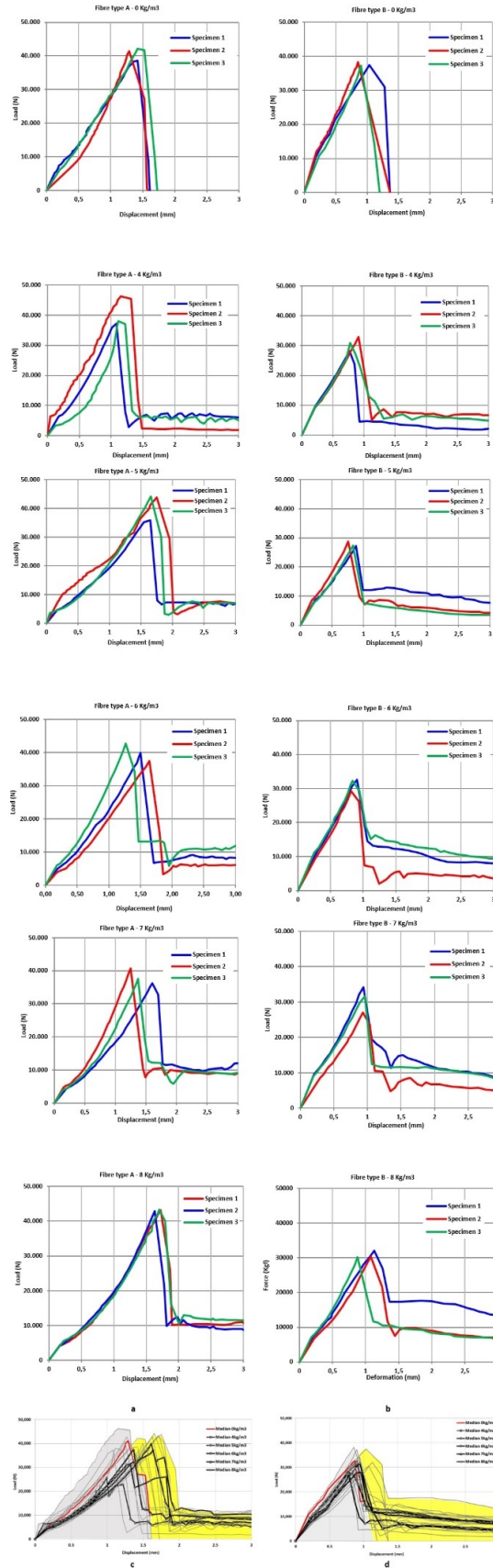


(c)

**Figure 6:** (a) Variation of indirect tensile strength in specimens with TYPE A fibre and TYPE B fibre, (b) specimen with fibre tested to indirect tensile, (c) specimen without fibre tested under indirect tension

### 3.6 Flexural Strength according to JSCE-SF-4

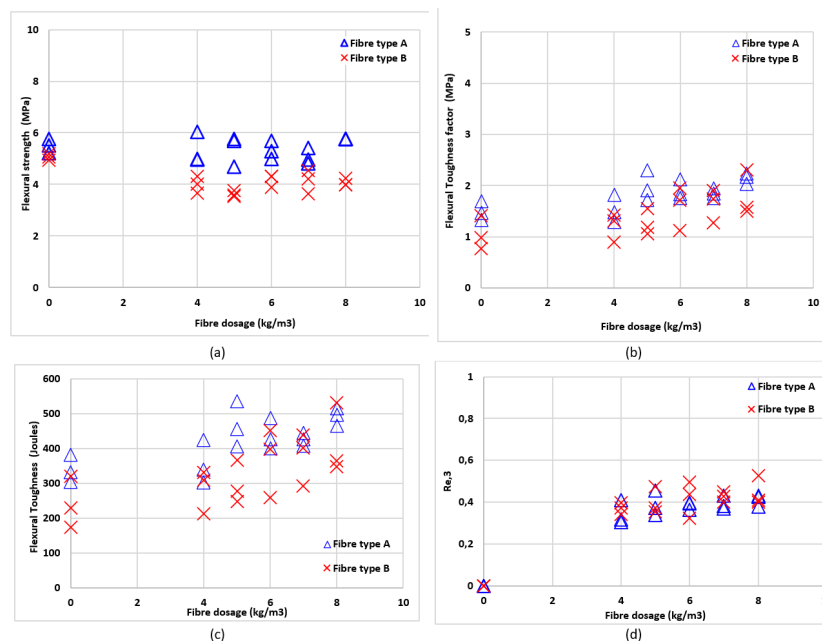
Figure 7a and 7b shows the Load-Displacement curves for the flexural strength test according to JSCE-SF-4 (1984) obtained for the different specimens in all their dosages for fibre types A and B respectively. The results obtained show that for both types of fibre, the mixture without added fibre experiences a sudden drop in strength when maximum flexural strength is reached. However, increasing fibre dosification achieves higher and higher residual strength and greater deformation capacity. Values close to 10000 N of residual resistance were obtained in both types of fibre. In addition, for the maximum dosage of 8 kgf/m<sup>3</sup>, resistance values greater than 10000 N are reached for fibre type A and near values to 20000 N are reached for fibre type B. The deformation values are doubled when the fibre is added regardless of its type. In Figure 7c and 7d, median values for each dosification are shown for fibre type A and fibre type B respectively. The gray areas show the dissipated area of the samples without fibre, and the yellow area shows the additional dissipated area when the fibres are used. As can be seen in said figures, the fibres provide inelastic incursion capacity and post-fracture resistance of concrete, reaching 25% post-fracture resistance of concrete in specimens with type A fibre and up to 47% resistance post-fracture of concrete in specimens with type B fibre. Additionally, a decrease in the slope can be observed in the elastic range, being more marked for type A fibre than for type B fibre.



**Figure 7. a:** Load vs. displacement in specimens tested according to JSCE-SF4 for Fibre TYPE A. **b:** Load vs. displacement in specimens tested according to JSCE-SF4 for Fibre TYPE B. **c:** Comparison of dissipated energy between specimens with fibre and without fibre according to JSCE-SF4 for Fibre TYPE A. **d:** Comparison of dissipated energy between specimens with fibre and without fibre according to JSCE-SF4 for Fibre TYPE B.

Figure 8a shows the flexural strength of the tested specimens. The flexural strength  $\sigma_b = P_{max}l/bh^2$  is obtained by dividing the maximum load and the length by the width and the height of the section squared. The results obtained show a slight decrease in the flexural strength of the specimens with fibre compared to the specimens without fibre. This corresponds to the results shown in Figures 7a and 7b, where the elastic stiffness in specimens without fibre reached higher stiffness than the specimens with fibre. Figure 8b shows the flexural toughness factor  $\bar{\sigma}_b = T_b l / \delta_{tb} b h^2$ , which is obtained by dividing the dissipated energy up to 3mm of deflection between the width and height of the section squared. This factor allows us to obtain the resistance associated with the ductility of the section according to the dosage of the fibre. The results obtained show an increase in the resistance as the dosage increases. Type A fibre shows a greater trend than type B fibre.

The dissipated energy is shown in figure 8c, where specimens with a greater quantity of fibre reach higher tenacity values, and the contribution of the fibre is evident. This energy also corresponds to the values reported in figures 7c and 7d, where the area in Yellow represents the increase in energy dissipated in fibre-reinforced concrete. Finally, figure 8d shows the results of the factor  $R_{e,3} = \bar{P}_{3mm} / P_{first,crack}$ , which represents a measure of ductility obtained as the average of the applied load up to 3mm of deflection divided by the load at which the first fracture is reached, according to TR34 (2013). The results obtained show that all the values are greater than 0.3 for both type A fibre and type B fibre, making it possible to use them in the polypropylene fibre reinforced concrete design using the procedures established in TR34 (2013) for concrete reinforced with steel fibres. Additionally, a trend of increasing  $R_{e,3}$  can be observed with increasing fibre dosage. Finally, type A fibre reached higher values of  $R_{e,3}$  than type B fibre, especially when the fibre dosage is greater than 5 kg/m<sup>3</sup>.



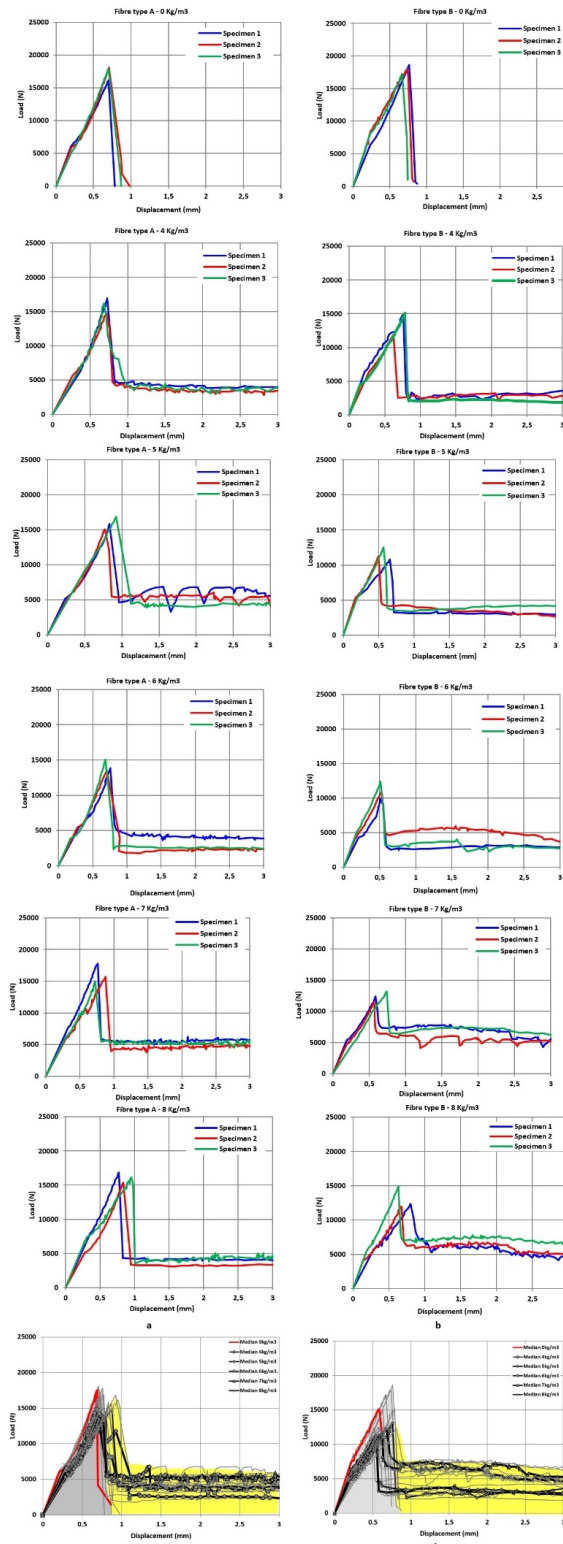
**Figure 8:** (a) Flexural strength of specimens tested according to JSCE-SF4 (1984), (b) Flexural toughness factor of specimens tested according to JSCE-SF4 (1984), (c) Flexural toughness of specimens tested according to JSCE-SF4 (1984) and (d)  $R_{e,3}$  parameter used in the design of slabs on ground.

### 3.7 Flexural Strength according to ASTM C1609

Figure 9a and 9b shows the Load-Displacement curves for the flexural strength test according to ASTM C1609 obtained for the specimens with dosages before mentioned for fibre types A and B respectively. The results obtained show that for both types of fibre, the mixture without added fibre experiences a sudden drop in strength when maximum flexural strength is reached. Similarly, to specimens tested according to JSCE-SF4, the specimens with fibre achieves higher residual strength and greater deformation capacity. Values close to 5000 N of residual resistance were obtained in case of Fibre type A and values with range between 2700-7500 N were reached in case of fibre type B.

In Figure 9c and 9d, median values for each dosification are shown for fibre type A and fibre type B respectively. The gray areas show the dissipated area of the samples without fibre, and the yellow area shows the additional dissipated area when the fibres are used. As can be seen in said figures, the fibres provide inelastic incursion capacity and post-fracture resistance of concrete, reaching 20% post-fracture resistance of concrete in specimens with type A fibre and up to 41% resistance post-fracture of concrete in specimens with type B fibre. Additionally, a decrease in the slope in the

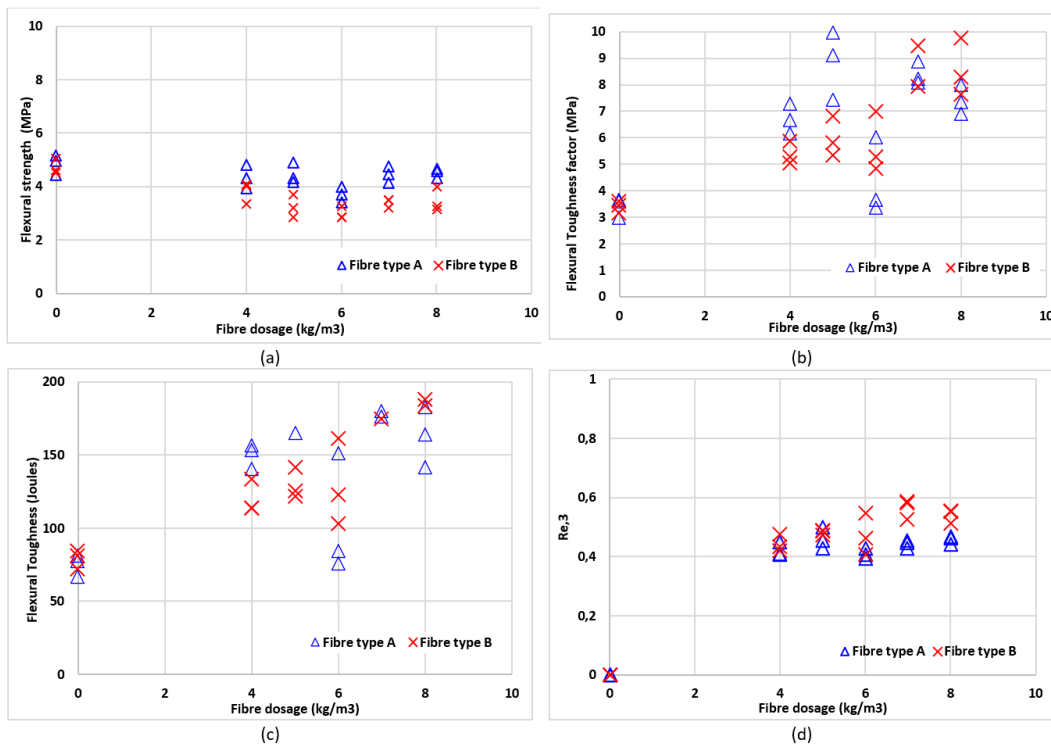
elastic range can be observed, being more marked for type B fibre with respect to type A fibre (otherwise than the tests performed according to JSCE- SF4).



**Figure 9a:** Force vs. deformation in flexural test specimens according to ASTM C1609 for fibre TYPE A. **b:** Force vs. deformation in flexural test specimens according to ASTM C1609 for fibre TYPE B. **c:** Comparison of dissipated energy between specimens with fibre and without fibre according to ASTM C1609 for Fibre TYPE A. **d:** Comparison of dissipated energy between specimens with fibre and without fibre according to ASTM C1609 for Fibre TYPE B.

Figure 10a shows the flexural strength of the tested specimens. The flexural strength was obtained with the same procedure where  $\sigma_b = P_{max}l/bh^2$  is obtained by dividing the maximum load and the length by the width and the height of the section squared. The results obtained show a slight decrease in the flexural strength of the specimens with fibre compared to the specimens without fibre. This variation corresponds to the results shown in Figures 9a and 9b, where the elastic stiffness in specimens without fibre reached higher stiffness than the specimens with fibre. Figure 10b shows the flexural toughness factor  $\bar{\sigma}_b = T_b l / \delta_{tb} b h^2$ , which is obtained by dividing the dissipated energy up to the 3mm deflection between the width and height of the section squared (ASTM C1609 does not require this value). The results obtained show an increase in Resistance as the dosage increases.

The dissipated energy is shown in figure 10c, where specimens with a greater quantity of fibre reach higher tenacity values, and the contribution of the fibre is evident. This result also corresponds to the values reported in figures 9c and 9d, where the area in Yellow represents the increase in energy dissipated in fibre-reinforced concrete. Finally, figure 10d shows the results of the factor  $R_{e,3} = \bar{P}_{3mm} / P_{first,crack}$ , which represents a measure of ductility obtained as the average of the applied load up to 3mm of deflection divided by the load at which the first fracture is reached, according to TR34 (2013). The results obtained show that all the values are greater than 0.4 for both type A fibre and type B fibre, being possible to use them in the reinforced concrete design with polypropylene fibre using the procedures established in TR34 (2013) for concrete reinforced with steel fibres. Additionally, a trend of increasing  $R_{e,3}$  can be observed with increasing fibre dosage. Finally, type B fibre reached higher values of  $R_{e,3}$  than type A fibre.

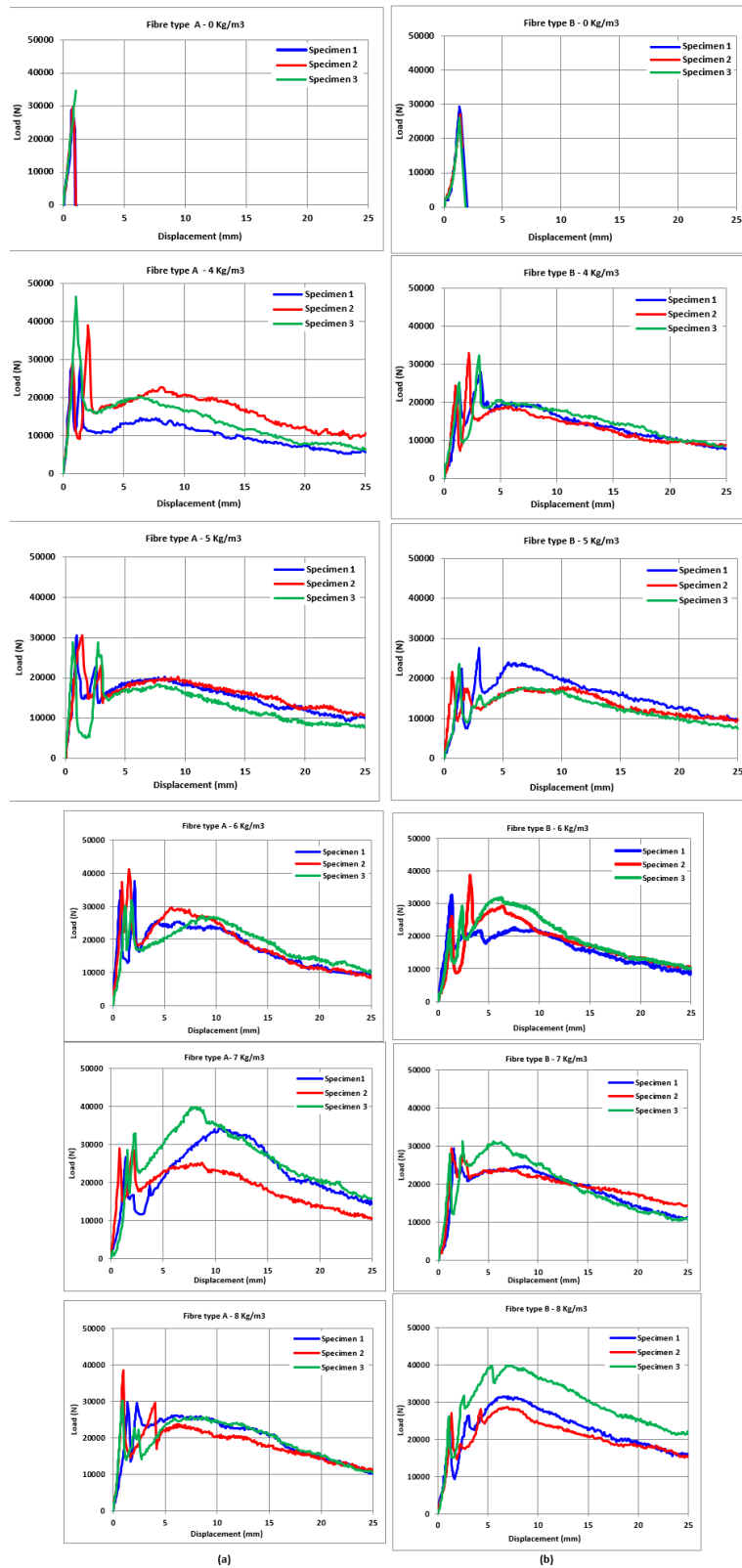


**Figure 10:** (a) Flexural strength of specimens tested according to ASTM C1609, (b) Flexural toughness factor of specimens tested according to ASTM C1609, (c) Flexural toughness of specimens tested according to ASTM C1609 and (d)  $R_{e,3}$  parameter used in the design of slabs on ground.

### 3.8 Energy absorption according to EFNARC

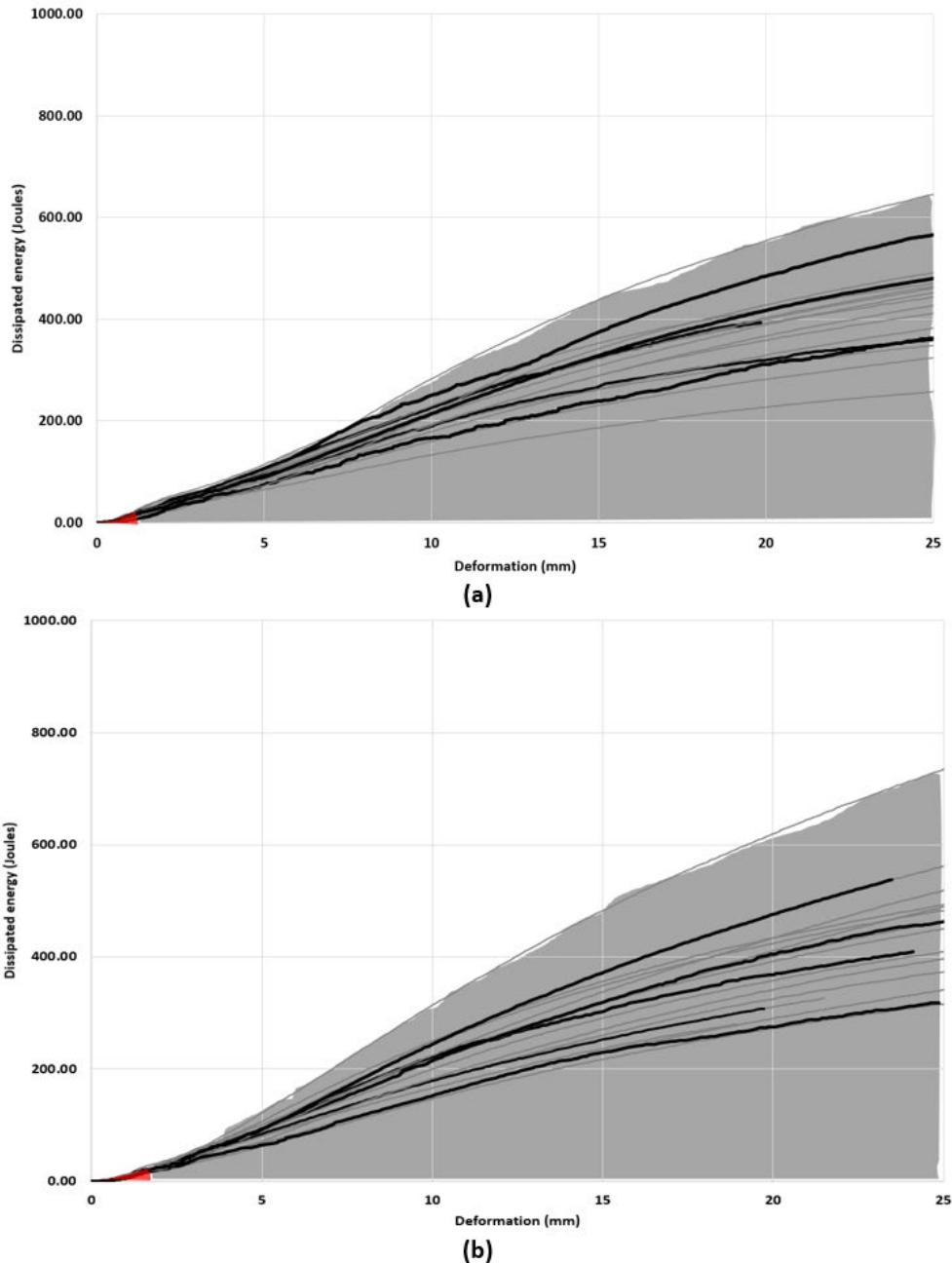
Figure 11a shows the load-displacement curve for the specimens without fibre and fibre type A, according to EFNARC (1996). The results obtained show that when a concrete specimen without fibre is tested, a maximum resistance of close to 36774 N is reached. However, for fibre type A dosages of 4 and 5 kg/m³ the residual resistance reaches up to 19613 N and a permanent deformation 20 times greater than the standard sample occurs. For fibre type A dosages of 6 and 8 kg/m³, a residual resistance of 29419 N and 24500 N respectively was registered, while the sample for 7 kg/m³ reached a residual resistance of 39226 N, exceeding the resistance of the standard sample. In Figure 11b, the load-displacement curve for the specimens without fibre and fibre type B, according to EFNARC (1996). The results obtained show that when a concrete specimen without fibre is tested, a maximum resistance of close to 29419 N is reached. However, for the dosages of 4 kg/m³ and 5 kg/m³, the residual resistance reaches up to 19613 N and a permanent

deformation 20 times greater than the standard sample. For dosages of 6 kg/m<sup>3</sup> and 7 kg/m<sup>3</sup>, a residual resistance of 29419 N was registered. In comparison, the sample for 8 kg/m<sup>3</sup> reached a residual resistance of 39226 N, exceeding the resistance of the standard sample and modifying a behavior from the peak with fall to a non-linear behavior with no obvious peak.



**Figure 11:** (a) Load vs. Displacement curve in specimens tested with TYPE A fibre according to EFNARC (1996) and (b) Load vs. Displacement curve in specimens tested with TYPE B fibre according to EFNARC (1996).

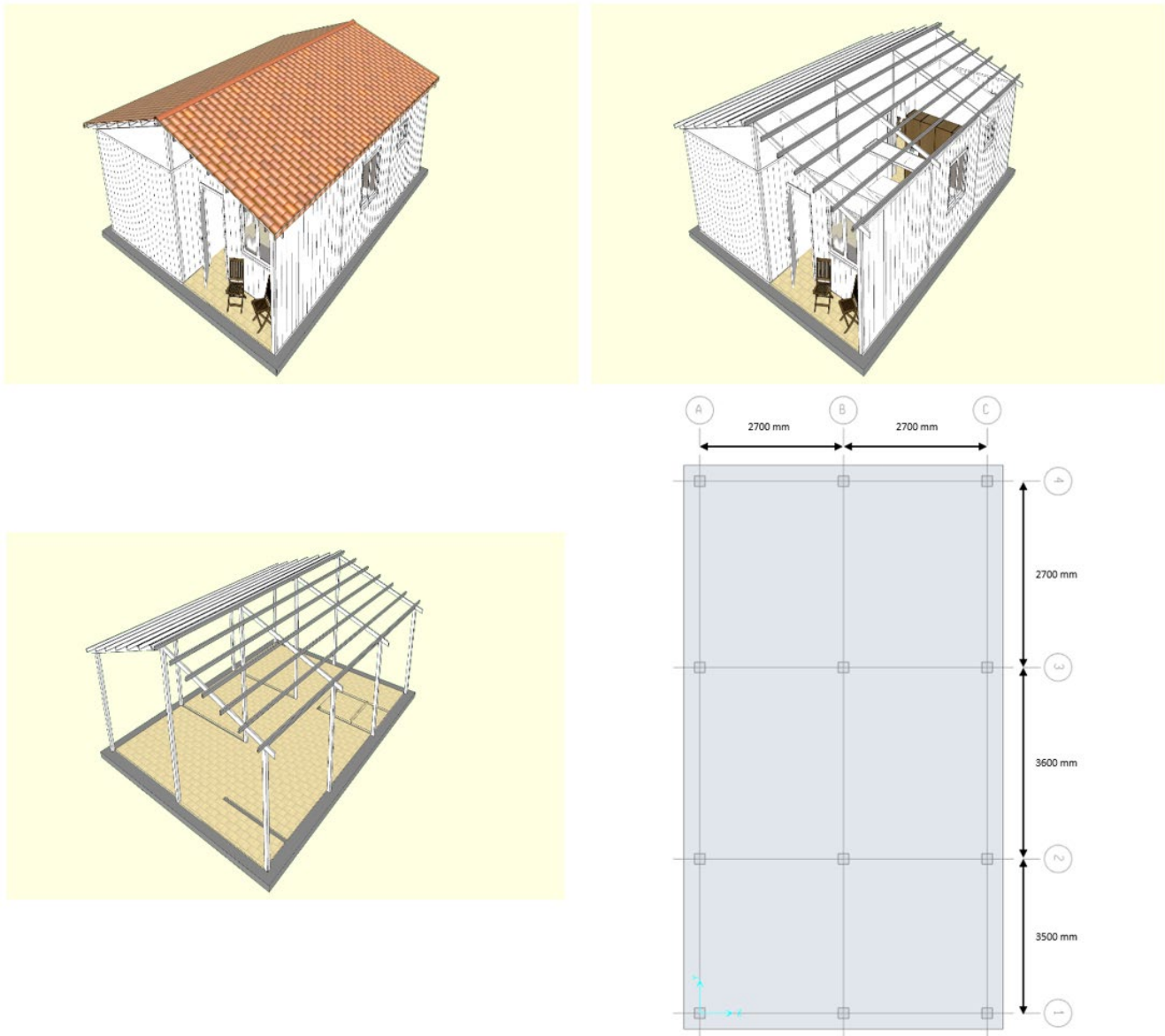
Figure 12 shows the dissipated energy obtained from Load vs. Displacement curves for both fibres. In figure 12a, the dissipated energy in specimens without fibre and fibre type A are reported. As can be seen in the figure 12a, the dissipated energy and the inelastic incursion capacity increase as the fibre dosage is increased. The red color shows the energy dissipated by the specimens without fibre. The lines in black color represent the median of each dosage, additionally observing that while the dosage increases, the tendency to increase energy is maintained. In figure 12b, the dissipated energy in specimens without fibre and fibre type B is shown. Specimens with type B fibre, in a similar way to type A fibre, as the fibre dosage increases, the dissipated energy and inelastic incursion capacity increases. Finally, it can be seen that fibre B is capable of dissipating more energy than fibre type B. This value is evidence of the effectiveness of the fibre to absorb tensile stresses derived from high levels of deformation, which improves the inelastic behavior of concrete.



**Figure 12:** (a) Dissipated energy vs. deformation in specimens tested with fibre type A according to EFNARC (1996) and (b) Dissipated energy vs. deformation in specimens tested with fibre type B according to EFNARC (1996).



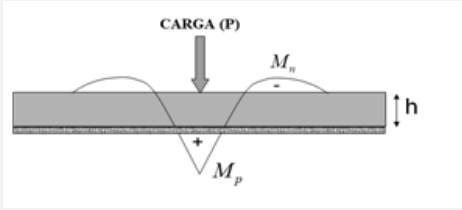
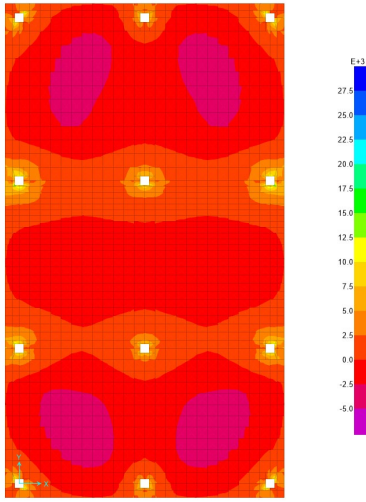
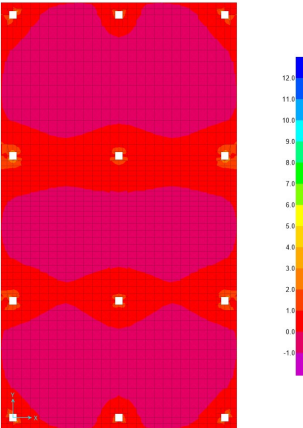
#### 4 APPLICATION IN THE DESIGN OF SLABS ON GROUND



**Figura 13:** Vista de la vivienda tipo usada para el diseño de la fundación.

In this research, the results obtained in the design of foundation slabs without reinforcing steel for one-level houses were applied. A schematic drawing of the typical house is shown in figure 13. The structural system of the house is made up of steel beams and columns supported on the foundation slab by support plates and anchor bolts. The roof is comprised of a lightweight deck and secondary beams to transfer loads to the Primary Element System. As shown in Figure 13, a total of 12 columns transmit the load to the Foundation System. Conventional design codes do not contemplate the use of polypropylene fibres for the structural design of slabs supported on the ground. However, in this research the use of the methodology proposed in ACI-360 (2010) is proposed to verify the Resistance flexural in industrial floors, use it in the flexural design of foundation slabs in buildings. In table 3, the design procedure is described.

Table 3: design procedure of design slabs on ground

Description	Formulation
1- For a load P (N), distributed in an area of 150x150mm and a concrete compression resistance of 21 (MPa), a Modulus of elasticity E (MPa) is obtained.	$P = 30,000 \text{ N}; A = 150 \times 150 = 22500 \text{ mm}^2 E = 4700 \sqrt{f_c} = 21538 \text{ MPa}$
2- Radius of effective stiffness L (mm), where h = 170 (mm) is the height of the section, u = 0.2 and K = 0.001 (N / mm <sup>3</sup> )	$L = \sqrt[4]{\frac{Exh^3}{12 * (1 - \nu^2)xK}} = 982 \text{ mm}$
3-The concrete modulus of rupture fr (MPa)	$f_r = 0.62 \sqrt{f_c} = 2.95 \text{ MPa}$
4- A distribution of bending moments is obtained according to the following drawing:	<p style="text-align: center;">Assuming a <math>R_{e,3} = 0.4</math> of fiber type A for a dosage of <math>6 \text{ kg/m}^3</math></p> $M_p = f_r x R_{e,3} x \frac{h^2}{6} x 1 \text{ mm} = 5472 \text{ N} \cdot \text{mm}$ $M_n = f_r x \frac{h^2}{6} x 1 \text{ mm} = 13690 \text{ N} \cdot \text{mm}$
	
where the positive moment is Mp and the negative moment is Mn.	
5- A concentrated load P applied on the slab should not exceed the Resistance load $P_p$ , which is obtained using expressions by Theory of Yield Lines, according to Meyerhof (1962).	$P_p = 6x \left( 1 + \frac{2xa}{L} \right) x (M_p + M_n) = 134.79 \text{ kN}$
6- Since $P_p > P$ , it is suitable.	$P_p > P; \text{ok}$
7-Comparing with a model in FE with the same load hypotheses and properties described above, the following distribution of moments $M_p$ can be obtained, where the reported values are less than 5472 N.mm	
8- Comparing with a model in FE with the same load hypotheses and properties described above, the following stress distribution can be obtained at the lower edge of the slab, where $\sigma < \sigma_{fr}$	

## 5 CONCLUSIONS

In this research, an experimental study was carried out to determine the influence of monofilament-type polypropylene fibres in concrete mixtures, from the quantification of resistance parameters such as compressive strength, tensile strength, flexural strength, and energy absorption, in two types of fibre from the SIKA company. A total of 180 specimens were tested, which allowed to obtain the following conclusions:

1. In the fresh state, the addition of polypropylene fibres shows that the fibres can affect the workability of the concrete mix. Therefore, it is a parameter to consider when the fibres are specified.
2. Compressive strength and tensile strength were not modified in specimens with fibre. However, the failure form is modified from a brittle failure mechanism to a more ductile mechanism. This variation is due to the connection between the cementitious matrix and the fibre filaments, providing inelastic capacity and post-fracture resistance of the concrete.
3. It is possible to replace the flexural reinforcing steel in floor-supported slabs of one-level homes with concrete reinforced with polypropylene fibres.
4. Flexural strength is not affected by the presence of fibres. However, the toughness increases as the dosage increases, reaching up to 50% more toughness, and the deformability is approximately twice that of a sample without fibre.
5. The energy absorption capacity is directly related to the dosage of fibre in the concrete mix. Specifically, it was obtained that the higher the fibre dosage, the greater the tenacity of the sample and, therefore, the greater the ability to resist tensile stresses, providing deformation capacity after cracking.
6. The performance achieved by both fibres is similar. However, TYPE A fibre reached its maximum performance for a dosage of 6 kg/m<sup>3</sup> and TYPE B fibre reached its maximum performance for a dosage of 8 kg/m<sup>3</sup>.
7. The  $R_{e,3}$  factor obtained ranges between 0.30 and 0.57, although technical documents for design recommend that the fibre to be used has a  $R_{e,3} \geq 0.3$ . However, these values are different according to the test methods used despite complying with similar experimental setups. The values in range of 0.4 - 0.6 were obtained according to ASTM C1609 and in range of 0.3 – 0.57 according to SCE-SF4 were obtained.

**Author's Contributions:** Conceptualization, Eduardo Nuñez-Castellanos; Ronald Torres-Moreno; Methodology, Eduardo Nuñez-Castellanos; Ronald Torres-Moreno; Software, Salvador Ligas-Fonseca; Eduardo Nuñez-Castellanos; Validation, Ronald Torres-Moreno; Eduardo Nuñez-Castellanos; Formal analysis, Salvador Ligas-Fonseca; Eduardo Nuñez-Castellanos; Ronald Torres-Moreno; Investigation, Ronald Torres-Moreno; Eduardo Nuñez-Castellanos; Salvador Ligas-Fonseca; Writing - Original Draft, Eduardo Nuñez-Castellanos; Writing - Review & Editing, A Roco-Videla; Nelson Maureira-Carsalade; Eduardo Nuñez-Castellanos; Visualization, A Roco-Videla; Eduardo Nuñez-Castellanos; Guillermo Bustamante-Laissle; Nelson Maureira-Carsalade; Supervision, Ronald Torres-Moreno; Guillermo Bustamante-Laissle; Nelson Maureira-Carsalade; Project administration, Eduardo Nuñez-Castellanos; Guillermo Bustamante-Laissle.

**Editor:** Marcílio Alves.

## 6 References

- Abdelmajeed, W. (2020). Evaluation of hybrid fibre-reinforced concrete slabs in terms of punching shear. *Construction and Building Materials*, 260, 119763.
- ACI 318-14. (2014). *Building Code Requirements for Structural Concrete and Commentary on Building Code Requirements for Structural Concrete*. Farmington Hills, MI: American Concrete Institute.
- ACI 360-10 (2010). *Guide to design slabs on ground*. Farmington Hills, MI: American Concrete Institute.
- Aidarov, S., Mena, F., & de la Fuente, A. (2021). Structural response of a fibre reinforced concrete pile-supported flat slab: full-scale test. *Engineering Structures*, 239, 112292.
- Amin, A., Foster, S. J., Gilbert, R. I., & Kaufmann, W. (2017). Material characterisation of macro synthetic fibre reinforced concrete. *Cement and Concrete Composites*, 84, 124-133.

- ASTM C1064/C1064M (2017). Standard Test Method for Temperature of Freshly Mixed Hydraulic-Cement Concrete. ASTM International, West Conshohocken, PA.
- ASTM C138/C138M (2019). Standard Test Method for Density (Unit Weight), Yield, and Air Content (Gravimetric) of Concrete. ASTM International, West Conshohocken, PA.
- ASTM C143/C143M (2020). Standard Test Method for Slump of Hydraulic-Cement Concrete. ASTM International, West Conshohocken, PA.
- ASTM C1609/C1609M (2019). Standard Test Method for Flexural Performance of Fiber-Reinforced Concrete (Using Beam with Third-Point Loading). ASTM International, West Conshohocken, PA.
- ASTM C231/C231M (2017). Standard Test Method for Air Content of Freshly Mixed Concrete by the Pressure Method. ASTM International, West Conshohocken, PA.
- ASTM C39/C39M (2020). Standard Test Method for Compressive Strength of Cylindrical Concrete Specimens. ASTM International, West Conshohocken, PA.
- ASTM C496/C496M (2017). Standard Test Method for Splitting Tensile Strength of Cylindrical Concrete Specimens. ASTM International, West Conshohocken, PA.
- Baarimah, A. O., & Moshin, S. M. S. (2017). Behaviour of reinforced concrete slabs with steel fibers. *Materials Science and Engineering*, 271, 012099.
- Cajka, Radim, Zuzana Marcalikova, Marie Kozielova, Pavlina Mateckova, and Oldrich Sucharda. (2020a). Experiments on Fiber Concrete Foundation Slabs in Interaction with the Subsoil. *Sustainability*, 12, 9: 3939.
- Cajka, Radim, Zuzana Marcalikova, Vlastimil Bilek, and Oldrich Sucharda. (2020b). Numerical Modeling and Analysis of Concrete Slabs in Interaction with Subsoil. *Sustainability*, 12, 23: 9868.
- Camille, C., Hewage, D. K., Mirza, O., Mashiri, F., Kirkland, B., & Clarke, T. (2020). Performance behaviour of macro-synthetic fibre reinforced concrete subjected to static and dynamic loadings for sleeper applications. *Construction and Building Materials*, 121469.
- Costa, C., Cerqueira, A., Rocha, F. & Velosa, A. (2018). The sustainability of adobe construction: past to future. *International Journal of Architectural Heritage*. 1-9
- EFNARC (1996), European Specification for Sprayed Concrete. European Federation of National Associations of Specialist Contractors and Material Suppliers for the Construction Industry, 30 pp.
- Fan, J., Shen, A., Guo, Y., Zhao, M., Yang, X., & Wang, X. (2020). Evaluation of the shrinkage and fracture properties of hybrid Fiber-Reinforced SAP modified concrete. *Construction and Building Materials*, 256, 119491.
- Fantilli, A. P., Orfeo, B., & Pérez Caldentey, A. (2021). The deflection of reinforced concrete beams containing recycled steel fibers. *Structural Concrete*.
- Hao, Y., & Hao, H. (2013). Dynamic compressive behaviour of spiral steel fibre reinforced concrete in split Hopkinson pressure bar tests. *Construction and Building Materials*, 48, 521-532.
- JSCE-SF-4 (1984). Method of test for flexural strength and flexural toughness of steel fiber reinforced concrete. Japan Concrete Institute, Tokio, Japan.
- Junaid, M., Saleem, S. M., Wu, Y. F., Lin, X., & Ríaz, M. (2021). Axial Stress-Strain Performance of Recycled Aggregate Concrete Reinforced with Macro-Polypropylene Fibres. *Sustainability*, 13(10), 5741.
- Mendoza, C., Aire, C., & Dávila, P. (2011). Influencia de las fibras de polipropileno en las propiedades del concreto en estados plástico y endurecido. *Concreto y cemento. Investigación y desarrollo*, 2(2), 35-47.
- Meyerhof, G. G. (1962). Load carrying capacity of concrete pavements. *Journal of Soil and Mechanics and Foundations Division, ASCE*, June, 89-117.
- Nana, W. S. A., Tran, H. V., Goubin, T., Kubisztal, G., Bennani, A., Bui, T. T., Cardia, A. & Limam, A. (2021, August). Behaviour of macro-synthetic fibers reinforced concrete: Experimental, numerical and design code investigations. In *Structures* (Vol. 32, pp. 1271-1286). Elsevier.

- Nogales, A., & de la Fuente, A. (2021). Numerical-aided flexural-based design of fibre reinforced concrete column-supported flat slabs. *Engineering Structures*, 232, 111745.
- TR34 (2013). The Concrete Society: Concrete industrial ground floors – a guide to design and construction. 4rd ed. Technical Report 34.
- Usman, M. (2020). Experimental investigation on durability characteristics of steel and polypropylene fiber reinforced concrete exposed to natural weathering action. *Construction and Building Materials*, 250, 118910.
- Wang, S., Zhang, M. H., & Quek, S. T. (2012). Mechanical behavior of fiber-reinforced high-strength concrete subjected to high strain-rate compressive loading. *Construction and Building Materials*, 31, 1-11.
- Wang, Y., Shao, X., Cao, J., Zhao, X., & Qiu, M. (2021). Static and fatigue flexural performance of ultra-high performance fiber reinforced concrete slabs. *Engineering Structures*, 231, 111728.
- Xu, H., Shao, Z., Wang, Z., Cai, L., Li, Z., Jin, H., & Chen, T. (2020). Experimental study on mechanical properties of fiber reinforced concrete: Effect of cellulose fiber, polyvinyl alcohol fiber and polyolefin fiber. *Construction and Building Materials*, 261, 120610.
- Zheng, D., Song, W., Fu, J., Xue, G., Li, J., & Cao, S. (2020). Research on mechanical characteristics, fractal dimension and internal structure of fiber reinforced concrete under uniaxial compression. *Construction and Building Materials*, 258, 120351.
- Zollo, R. F. (1997). Fiber-reinforced Concrete: An Overview after 30 Years of Development. *Cement and Concrete Composites*, 19, 107-122